VII Brazilian Symposium on Rock Mechanics – SBMR 2016
Rock Mechanics and Rock Engineering for Innovation and Development
ISRM Specialized Conference 19-22 October, Belo Horizonte, Minas Gerais, Brazil

A New Model to Predict and Quantify Sand Production for Unconsolidated and Low Consolidated Reservoirs

Edson Felipe Araujo Guerrero
Universidad Nacional de Colombia, Medellin, Colombia, efaraujog@unal.edu.co

Alejandra Arbelaez Londoño
Universidad Nacional de Colombia, Medellin, Colombia, aarbelal@unal.edu.co

Yurladys Cross Arroyave
Universidad Nacional de Colombia, Medellin, Colombia, ycrossa@unal.edu.co

Guillermo Alzate Espinosa
Universidad Nacional de Colombia, Medellin, Colombia, gaalzate@unal.edu.co

Abel Naranjo Agudelo
Universidad Nacional de Colombia, Medellin, Colombia, anaranjo@unal.edu.co

SUMMARY: Many of world oil reserves are stored in Heavy Oil reservoirs, which have low levels of consolidation and deform permanently under the influence of mechanical stresses. During Heavy Oil production, the mechanical stability of the reservoir is affected by different factors such as the fluid flow, current stresses regime, rock strength, completion type, water intrusion among others, which can cause sand production. This phenomenon occurs in many of the exploitation processes performed in an oil well and is a relevant factor in problems related with wellbore and surface equipment damage, wellbore stability, and reservoir productivity, among others. It has widely seen that these reservoirs behave mechanically in an elastoplastic way, in which rock strains can be of both types, elastic and plastic. Many investigations are focused on determining the onset of sand production, but few attempt are made to quantify the amount of produced sand according to the phenomenology of the problem. In order to predict and quantify the produced sand, a 3D single well numerical model is developed solving the single-phase fluid flow coupled with geomechanics for a reservoir with elastoplastic behavior, which uses the Mohr Coulomb failure criterion. This model emphasizes on the effects near wellbore and integrates a sand erosion criterion as a function of the rock plastic strain and the fluid flow velocity. The entire model takes into account changes in the porosity and permeability as a function of effective stresses, strains and produced sand mass. Initially, an experimental sand production test is studied for understanding of the phenomena involved in the sand production events, and then the results' test are modeled and matched using the numerical model presented in this article. First, the experimental test is modeled matching its mechanical behavior as a function of the measured data in the test and the rock properties. Then, the experimental sand production is modeled using the proposed sand production criterion. The obtained results exhibit a good match especially between the experimental and the modeled sand production. Also as results, petrophysical variables such as porosity and permeability are highly affected by strain and sand production, highlighting the relevance of this type of models. Although this model shows a high complexity, it allows a further analysis of the related variables and thus to visualize options to increase hydrocarbon production by harnessing the potential of this type of reservoirs.

KEYWORDS: Sand production, numerical model, elastoplastic behavior, Heavy Oil reservoirs.

1 INTRODUCTION

Poorly or non-consolidated reservoirs are usual to find in Heavy Oil reservoir, which behave mechanically in an elastoplastic way showing very important irreversible deformations during drilling, completion and production operations. Sand production is a phenomenon found almost in every poorly or non-consolidated reservoir and it can cause serious problems both in borehole and in surface equipment. Some problems involve perforations and well plugging, equipment damage due to the abrasive nature of the sand grains among others. Cleaning sanded wells or changing periodically the well facilities result in high remediation costs. Thus, sand production is a costly problem and therefore many companies use to implement mechanical methods to reduce the sanding intensity by using gravel pack, slotted liner, resins injection or other technologies. Thereby, it is important to mention that these technologies reduce the well conductivity when trying to prevent sand production.

Rahmati, et al. (2013) underlined the need to understand clearly the sand production phenomenon with the intention to prevent operation lags and to optimize reservoir production. During the understanding the sand production phenomenon, it is matter of time to come up with the picture of a highly complex problem that involves several variables interrelated, and is currently a topic of research interest. One of the main indicators that a producing reservoir is prone to produce sand is the strength of the formation open to hydrocarbons flow. This indicator is measured with a Uniaxial Compressive Strength test (UCS) or with a Thick Walled Cylinder test (TWC) and helps to understand the stress intensity level that the formation is able to stand before yielding.

A second indicator for the sand production is the in-situ stress regime acting over the reservoir. This indicator is important because it defines the stress intensity level to which the formation will be subjected during all the operations. Coupled with it are the reservoir pressure level and the pressure drop around the well, which are the reason of the changes in effective stresses at the wellbore face and inside the reservoir. Other but not less important indicators that have proved importance in sand production phenomenon are: the weakening effect due to water intrusion, the well completion and path, cyclical production and injection operations, the hammer effect among others.

In this work, it is presented a 3D single well numerical model to solve the single-phase fluid flow coupled with geomechanics for a reservoir with an elastoplastic behavior, which uses the Mohr Coulomb failure criterion. This is able to predict and quantify the sand produced because it integrates a sand erosion criterion, which is a function of the rock plastic strain and the fluid flow velocity. The entire model takes into account changes in the porosity and permeability as a function of effective stresses, strains and produced sand mass. The experimental validation of the model is presented, included the quantified sand production based on experimental data.

2 CONCEPTUAL FRAMEWORK

2.1 Constitutive Relationship

Initially, for modeling the rock mechanical behavior an elastic constitutive model accordingly to Hooke's Law is used. It relates directly the deformations induced in the material with the response in stresses. Based on the elastic assumption, all the material deformations are reversible and material can recover its initial configuration.

Hooke's law for porous materials includes the pressure of the fluids inside the rock. This can be expressed as follows:

$$\sigma_{ij} = 2\mathrm{G}\varepsilon_{ij}{}^{\mathrm{e}} + (\lambda\varepsilon_{kk}{}^{\mathrm{e}} + \alpha p)\delta_{ij} \qquad (1)$$

Being σ_{ij} the stress tensor, ε_{ij} the elastic deformation, p the fluid pressure inside the porous spaces, and α the Biot's coefficient. In this equation, the relationship between stresses, deformations and pore pressure is linear. Besides, the convention used is that compressive stresses are positive.

However, low or non-consolidated formations can show a permanently deformed shape after a load cycle. It means that this material are not behaving elastically at all. The permanent deformations found after loading cycles are inelastic deformations and to model these deformations some constitutive models are used. One of the approximations is the use of elastoplastic constitutive models. For the development of this work, an elastoplastic constitutive model based on Mohr Coulomb yielding theory is used.

For the plastic deformation calculation, the Mohr Coulomb failure criterion is used. The failure envelope in function of main effective stresses (σ'_i) is defined in Eq.2.

$$f^{\mathrm{shear}} = -\sigma'_1 + \sigma'_3 \mathrm{N}_\varphi + 2\mathrm{S_o}\sqrt{\mathrm{N}_\varphi} \qquad (2)$$

When the material under study is submitted to a loading, initially the material will behave elastically, but when the stress state reaches the failure envelope ($f^{\mathrm{shear}} = 0$), then it is said that the material started to yield and will deform plastically (Figure 1).

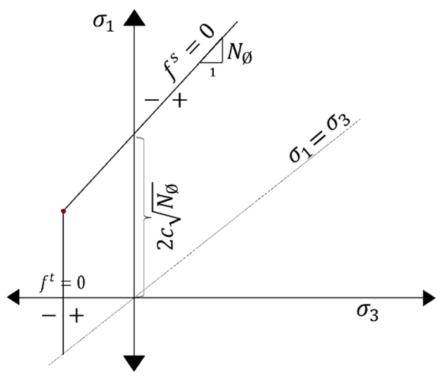

Figure 1. Mohr Coulomb failure envelope (f^{shear}) and tension envelope (f^{tensile}).

The calculations of plastic deformations are obtained using Eq. 3 - 5, which in this case is a non-associated flow rule.

$$\dot{\varepsilon}_{ij}{}^{\mathrm{p}} = \bar{\lambda}\frac{\partial g^{\mathrm{shear}}}{\partial \sigma_{ij}} \qquad (3)$$

$$g^{\mathrm{shear}} = -\sigma'_1 + \sigma'_3 \mathrm{N}_\Psi \qquad (4)$$

$$\mathrm{N}_\Psi = \frac{1+\sin\Psi}{1-\sin\Psi} \qquad (5)$$

To quantify the level of plastic deformations experienced by the material, we implement an indicator of shear plastic deformation level Eq.6.

$$\dot{\varepsilon}^{\mathrm{ps}} = \left\{\frac{\left(\dot{\varepsilon}_1^{\mathrm{p}}-\dot{\varepsilon}_{\mathrm{m}}^{\mathrm{p}}\right)^2+\left(\dot{\varepsilon}_2^{\mathrm{p}}-\dot{\varepsilon}_{\mathrm{m}}^{\mathrm{p}}\right)^2+\left(\dot{\varepsilon}_3^{\mathrm{p}}-\dot{\varepsilon}_{\mathrm{m}}^{\mathrm{p}}\right)^2}{2}\right\}^{\frac{1}{2}} \qquad (6)$$

Being,

$$\dot{\varepsilon}_{\mathrm{m}}^{\mathrm{p}} = \frac{\left(\dot{\varepsilon}_1^{\mathrm{p}}+\dot{\varepsilon}_2^{\mathrm{p}}+\dot{\varepsilon}_3^{\mathrm{p}}\right)}{3} \qquad (7)$$

2.2 Model Definition

In order to define the behavior of fluid flow through the porous medium for sand production analysis, the fluid mass balance in a differential element is used (Eq.8). Likewise, the formation matrix undergoes changes as a function of current stresses, plastic deformation and sand production, so the solid mass balance equation is also used (Eq.9).

$$-\nabla\cdot(\rho_{\mathrm{f}} v_{\mathrm{f}} \phi) = \frac{\partial(\rho_{\mathrm{f}}\phi)}{\partial t} \qquad (8)$$

$$-\nabla\cdot(\rho_{\mathrm{s}}(1-\phi) v_{\mathrm{s}}) = \frac{\partial(\rho_{\mathrm{s}}(1-\phi))}{\partial t} \qquad (9)$$

Chen, et al. (1995) showed the way to couple geomechanics and fluid flow for a porous medium with mechanical deformation. Based in their work, we can express:

$$\nabla\cdot v_{\mathrm{s}} = -\frac{1}{V_{\mathrm{s}}}\frac{\mathrm{d}V_{\mathrm{s}}}{\mathrm{d}t} + \frac{1}{V_{\mathrm{b}}}\frac{\mathrm{d}V_{\mathrm{b}}}{\mathrm{d}t} \qquad (10)$$

Note that Eq. 10 is a statement of the solid mass balance from Eq. 9. The V_{s} term in Eq. 10 is the solid volume. The solid volume change with time depends on the solid compressibility (which is always a low value) or in the eroded solid mass (sand production case). The term V_{b} is the bulk volume. If the solid volume change is expressed as a function of the eroded sand rate, then,

$$\frac{1}{V_s}\frac{dV_s}{dt} = -\frac{\dot{m}_s}{\rho_s V_b(1-\phi)} \quad (11)$$

Thus, the mass balance must fulfill, Eq. 12,

$$\nabla \cdot v_s = \frac{\dot{m}_s}{\rho_s V_b(1-\phi)} + \frac{1}{V_b}\frac{dV_b}{dt} \quad (12)$$

Introducing Darcy's law and the solid mass balance equation (Eq. 12), then the fluid mass balance equation (Eq. 8) results in:

$$\nabla \cdot \left(\frac{\rho k}{\mu}\nabla p\right) = \rho\phi\left[\frac{1}{\rho}\frac{d\rho}{dt} + \frac{1}{V_p}\frac{dV_p}{dt} + \frac{\dot{m}_s}{\rho_s V_b(1-\phi)}\right] \quad (13)$$

This expression is the differential fluid flow equation for a deformable porous media, which is producing sand. The rock strain nature should be defined because strain could be elastic or plastic.

The poroelastic behavior of a porous medium is well defined in Zimmerman, et al (1986). In this work, the porous medium only behaves elastically. Then, the porous volume change with time can be expressed as,

$$\frac{1}{V_p}\frac{\partial V_p}{\partial t} = \frac{1}{\phi}\left(c\frac{\partial p}{\partial t} - \alpha\frac{\partial \varepsilon_v{}^e}{\partial t}\right) \quad (14)$$

Being $\varepsilon_v{}^e$, the volumetric elastic deformation which for Zimmerman theory meets $\varepsilon_v{}^e = \varepsilon_v$ and c is defined as,

$$c = c_{bc} - (1+\phi)c_s - (c_{bc} - c_s)\alpha \quad (15)$$

To introduce the elastoplastic behavior on the expressions for the porosity volume increments, the following mathematical approach is presented. For a material with elastoplastic behavior, the change of the total volume is defined as the sum of the volume change by elastic deformation plus the volume change by plastic deformation, (Eq. 16).

$$dV_b = dV_b^p + dV_b^e \quad (16)$$

By using the definition of porosity, it can be expressed:

$$dV_p^p = dV_b^p - dV_s^p \quad (17)$$

For an elastoplastic material, the volumetric strain is the sum of plastic and elastic effects. Then, the plastic volumetric strain is:

$$d\varepsilon_v^p = -\frac{dV_b^p}{V_b} \quad (18)$$

Applying the same concept of volumetric deformation for the solid, Eq. 19 can be defined,

$$d\varepsilon_{vs}^p = -\frac{dV_s^p}{V_s} = -\frac{dV_s^p}{(1-\phi)V_b} \quad (19)$$

The plastic porous volume change can be obtained introducing Eq. 18 and 19 in Eq. 17.

$$dV_p^p = V_b\left[-d\varepsilon_v^p + (1-\phi)d\varepsilon_{vs}^p\right] \quad (20)$$

Eq. 20 can be rewritten to obtain the porous volumetric due to plastic strain, Eq. 21. This equation shows the dependency of porous volume with the plastic deformation. Notice that this result states that a plastic deformation induces a porous volume change.

$$d\varepsilon_{vp}^p = -\frac{dV_p^p}{V_p} = \frac{d\varepsilon_v^p - (1-\phi)d\varepsilon_{vs}^p}{\phi} \quad (21)$$

Thus, the porous volume change, expressed as function of pressure, stresses (elastic part) and volumetric plastic deformations are as follows,

$$\frac{dV_p}{V_p} = \frac{dV_p^e + dV_p^p}{V_p} = c_{pp}dp - c_{pc}d\sigma_m - d\varepsilon_{vp}^p \quad (22)$$

Using Eq. 22, the porous volume change in Eq. 13 results as,

$$\frac{1}{V_p}\frac{\partial V_p}{\partial t} = \frac{1}{\phi}\left(c\frac{\partial p}{\partial t} - \alpha\frac{\partial \varepsilon_v^e}{\partial t} - \frac{\partial \varepsilon_v^p}{\partial t}\right) \quad (23)$$

Where the deformation $d\varepsilon_s^p$ (the plastic volumetric deformation of the solid rock) is assumed zero because the plastic deformation in porous materials is more likely to generate cracks and spaces $(d\varepsilon_p^p)$, than to generate volume changes in the solid material. This effect is pronounced in unconsolidated formations.

Finally, introducing the sand production term, and assuming that all produced sand reflects an increase in porosity,

$$\frac{1}{V_p}\frac{\partial V_p}{\partial t} = \frac{1}{\phi}\left(c\frac{\partial p}{\partial t} - \alpha\frac{\partial \varepsilon_v^e}{\partial t} - \frac{\partial \varepsilon_v^p}{\partial t} + \frac{\dot{m}_s}{V_b \rho_s}\right) \qquad (24)$$

This equation allows performing the geomechanical couple with the fluid flow phenomena introducing the porous volume change due to both plastic and elastic strains, and including the sand production related porous volume changes.

For the mechanical model, the stresses equilibrium equation (Eq. 25) is solved. The term F_j is related with the body forces, which in this case are assumed negligible.

$$\sigma_{ij,j} + F_j = 0 \qquad (25)$$

To solve Eq. 13 and 25 an iteratively coupling is developed where the main variables to solve are pressure and displacements, the plastic correction and sand produced mass. The physical domain for the sand production model has a cylindrical shape with a hole in it as is shown in Figure 2. Under this model, several boundary conditions are applied. On the top, a displacement condition is defined to control the total axial deformation. While the top and bottom pressure conditions are of Von Neumann boundary type for defining no flow through this surfaces. For the radial inner and outer surfaces, a radial stress condition is defined for the mechanical model, and the value of the pressure is defined for the fluid flow model.

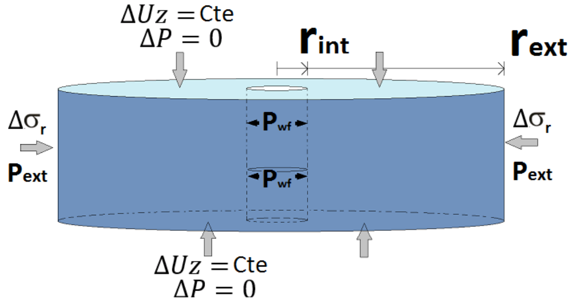

Figure 2. Physical domain of the sand production model, and boundary conditions.

2.3 Porosity and permeability.

Using the definitions presented in section 2.2, the porosity is calculated in Eq.26. Finally, permeability calculations are performed using the Carman Kozeny relationship.

$$d\phi = [c_{bc}(\phi - 1) + c_s][d\sigma_m - dp] - (1 - \phi)d\varepsilon_v^p + \frac{\phi \dot{m}_s}{V_b \rho_s}dt \qquad (26)$$

3 DATA AND OBSERVATIONS

The study is based on detailed experimental test presented by Nouri, et al. (2006). In this work, a well characterized sample is subjected to a test of sand production. The sample properties are presented in Table 1. This sample is a cylinder with an inner hole in it; and is subjected to a radial pressure gradient and to stresses in axial and radial directions, which are growing independently. The internal hole of the sample is subjected to atmospheric pressure throughout the test. The sand production rate is measured. The experimental test results are presented in Figure 3.

Table 1. Sample characterization. Taken from Nouri et al. (2006).

Property	Value
Young Modulus (Pa)	4E8
Poisson Ratio	0.438
Initial Porosity	0.36
Initial Permeability (m^2)	3.55E-12
Solid density (kg/m^3)	2670
Internal radius (m)	1.27E-2
External radius (m)	6.25E-2
Height (m)	0.25
UCS (Pa)	1.36E6
Friction Angle (°)	27.5
Dilation angle (°)	-7

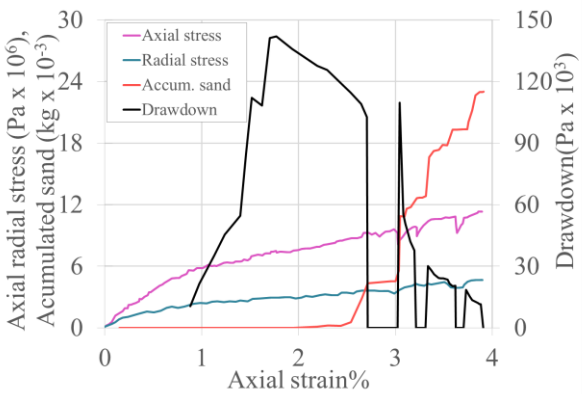

Figure 3. Results of the sand production test. Taken from Nouri et al. (2006).

With the data, the intention is to use the numerical model in modelling this test. An important feature is that experimental produced sand data as an input for the model. The axial total stress is the matching and comparing variable.

Several cases of modelling are analyzed. Initially, the model is applied for two different scenarios of mechanical behavior: an elastic behavior and an elastoplastic behavior, looking for addressing their main differences and impact in productivity (both without sand production).

Based on these simulations, the properties of porosity, permeability and stresses resulting in the sample at the end of the experimental test are compared and analyzed. Finally, a third case is defined, in which sand production is modeled based on the experimental test measurements.

4 RESULTS AND DISCUSSION

Figure 4 presents the comparison between the elastic and the elastoplastic modelling of the test. Notice the overestimation on the total axial stress calculations for the elastic case compared with the experimental results. For the case el elastoplastic modelling, it is important to mention that the UCS, friction angle and dilation angle are of great importance in the adjustment of this test because they control the onset of the plastic behavior. The complete matching study for the elastoplastic scenario is presented in Araujo, et al. (2015).

Based on Figure 4, it is good to mention that the elastoplastic constitutive relationship allows to model accurately the mechanical behavior of low or non-consolidated formations.

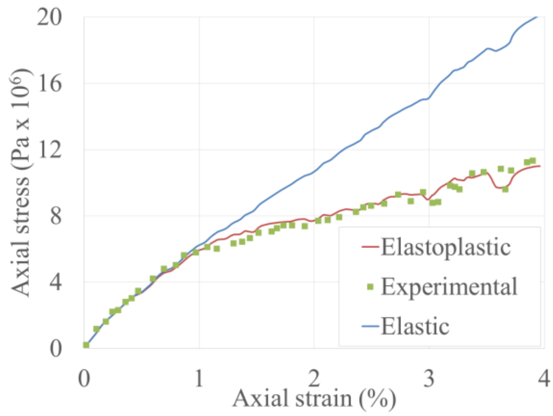

Figure 4. Mechanical behavior adjustment, elastic and elastoplastic comparison.

At the very end of the test, the sample concludes submitted to a load as a function of the generated stresses and deformations, i.e. at axial strain of 4%. At this final state, porosity and permeability inside all the sample is calculated for different radius. The final normalized porosity and permeability profiles in radial direction are presented in Figure 5 and 6, respectively. This graphs show these properties remain almost constant for the assumption of elastic behavior, but a big variation is found for the assumption of an elastoplastic behavior. Besides, a huge porosity and permeability increment is reached when produced sand is involved in the calculations.

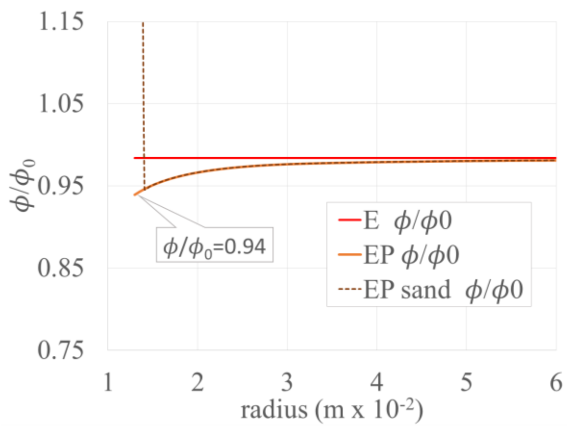

Figure 5. Porosity ratio profile for: elastic (E), elastoplastic (EP) and elastoplastic-Sand cases.

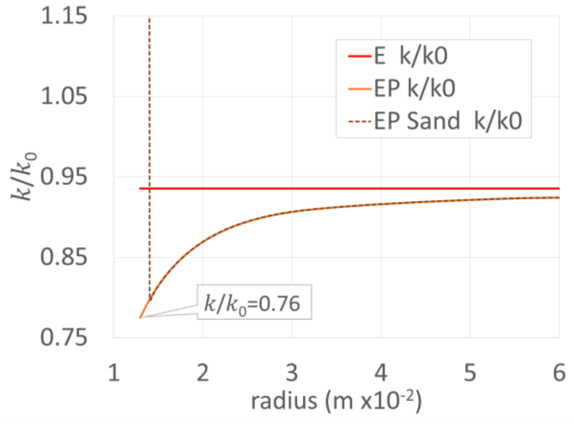

Figure 6. Permeability ratio profile for: elastic (E), elastoplastic (EP) and elastoplastic-Sand cases

CONCLUSIONS

A mathematical approach is presented to model the phenomenon of sand production coupling the pressure and stresses affecting the reservoir. This model consists of a module for fluid flow and a module for the mechanical behavior of the porous rock (reservoir). This model also introduces a new term for sand produced effect in porosity and permeability.

One of the main conclusion is that a mistaken assumption of the stress – strain constitutive relationship of the reservoir can cause large errors in the calculations of the porosity and permeability of the porous medium. It is shown that, for this case, the mechanical behavior is better modeled using an elastoplastic constitutive model than an elastic model. Assuming an elastic constitutive relationship implies an overestimation of the calculated axial stress.

Besides, it is very important to account for the porosity and permeability changes introduced by the behavior of the reservoir. As it was shown, these properties can change strongly in the wellbore face due to the elastoplastic behavior of the rock. Moreover, the sand production generates a big increment in porosity and permeability due to the sample erosion.

This study shows that this kind of model is able to predict the skin level around the wellbore, moreover to include the effects related to the sand production level in well conductivity. Then, with this tool, is possible to have a better understanding of the effect that production (fluid and sand), wellbore operations and interventions have over the productivity of a Heavy Oil reservoir.

ACKNOWLEDGEMENTS

The authors would like to thank to Colciencias and Ecopetrol for their trust and their financial support.

NOMENCLATURE

c : Compressibility (1/Pa)
f^{shear} : Shear Mohr Coulomb Function (Pa)
g^{shear} : Shear Plastic potential function (Pa)
G : Shear modulus (Pa)
k : Permeability (m^2)
m : Mass (kg)
p : Pressure (Pa)
q : Discharge rate (m/s)
t : Time (s)
S_o : Cohesion (Pa)
u : Displacement (m)
v : Velocity (m/s)
V : Volume (m^3)
α : Biot’s coefficient (dimensionless)
ε : Total strain (dimensionless)
λ : Lamé modulus (Pa)
$\bar{\lambda}$: Plastic multiplier (1/s)
μ : Fluid viscosity (Pa·s)
ρ : Density (kg/ m^3)
σ : Total Stress (Pa)
σ' : Effective stress (Pa)
δ Kronecker delta
ϕ : Porosity (dimensionless)
φ : Friction angle (°)
Ψ : Dilation angle (°)

SUPERTSCRIPTS

e : Elastic
p : Plastic
ep : Elastoplastic
ps : Plastic - Shear
s : Due to sand production
$\dot{x}$: Derivative of x with time

SUBSCRIPT

b : Bulk
bc : Bulk due to confining
f : Fluid
i : Index

j	:	Index
k	:	Index
p	:	Porous
pp	:	Porous due to pressure
pc	:	Porous due to confining
s	:	Solid
v	:	Volumetric
0	:	Initial value
$1, 2, 3$	:	Indices for main stresses or strains

REFERENCES

Araujo, E.F., Alzate, G.A., & Arbelaez, A. (2015). A Prediction and Quantification Model of Sand Production. Universidad Nacional de Colombia, Medellin,Colombia. *Proceedings of Heavy Oil Latin America Conference & Exhibition. Bogota, COL.*

Chen, H.-Y., Teufel, L. W., & Lee, R. L. (1995). Coupled Fluid Flow and Geomechanics in Reservoir Study - I. Theory and Governing Equations. *Proceedings of SPE Annual Technical Conference and Exhibition*, SPE, Dallas, TX, p. 507–519.

Nouri, A., Vaziri, H., Belhaj, H., & Islam, R. (2006). Sand-Production Prediction: A New Set of Criteria for Modeling Based on Large-Scale Transient Experiments and Numerical Investigation. *Proccedings of SPE Annual Technical Conference and Exhibition*, Houston, TX, USA, Vol.11 (no.2), p. 227–237.

Rahmati, H., Jafarpour, M., Azadbakht, S., Nouri, A., Vaziri, H., Chan, D., & Xiao, Y. (2013). Review of Sand Production Prediction Models. *Journal of Petroleum Engineering*, Vol. 2013, Article ID 864981, 16 p.

Zimmerman, W., Somerton, W. H., & King, M. S. (1986). Compressibility of Porous Rocks. *Journal of Geophysical Research*, 91(B12), p. 12765–12777.